Eur. Phys. J. B **6**, 225–231 (1998)

THE EUROPEAN PHYSICAL JOURNAL B

Tracer dispersion in power law fluids flow through porous media: Evidence of a cross-over from a logarithmic to a power law behaviour

V. Chaplain[1,a], C. Allain[2], and J.P. Hulin[2]

[1] Unité de Phytopharmacie et Médiateurs Chimiques, INRA, route de Saint-Cyr, 78026 Versailles Cedex, France
[2] FAST[b], Bâtiment 502, Campus Universitaire, 91405 Orsay Cedex, France

Received: 22 July 1997 / Revised and Accepted: 2 July 1998

Abstract. An analytical model is presented to describe the dispersion of tracers in a power-law fluid flowing through a statistically homogeneous and isotropic porous medium. The model is an extension of Saffman's approach to the case of non-Newtonian fluids. It is shown that an effective viscosity depending on the pressure gradient and on the characteristics of the fluid, must be introduced to satisfy Darcy's law. An analytical expression of the longitudinal dispersivity $\lambda_{//}$ is given as a function of the Peclet number Pe and of the power-law index n that characterizes the dependence of the viscosity on the shear rate ($\eta \propto \gamma^{n-1}$). As the flow velocity increases the dispersivity obeys an asymptotic power law: $\lambda_{//} \propto Pe^{1-n}$. This asymptotic regime is achieved at moderate Peclet numbers ($Pe \approx 10$) with strongly non-Newtonian fluids ($n \leq 0.6$) and on the contrary at very large values when n goes to 1 ($Pe \geq 10^4$ for $n = 0.9$). This reflects the cross-over from a scaling behaviour for $n \neq 1$ towards a logarithmic behaviour predicted for Newtonian fluids ($n = 1$).

PACS. 47.55.Mh Flows through porous media – 47.50.+d Non-Newtonian fluid flows

1 Introduction

Tracer dispersion in porous media is involved in many industrial processes as well as in environmental and biological issues [1,2]. Dispersion results from the combined action of molecular diffusion and convection, their relative importance being characterized by the Peclet number Pe ($Pe = Ud/D_m$ in which U and d are the characteristic velocity and grain size and D_m the molecular diffusion coefficient). In the diffusive regime ($Pe \ll 1$), dispersion only depends on molecular diffusion. On the contrary, in the convective regime, ($Pe \gg 1$), dispersion is dominantly governed by the velocity distribution inside the porous medium. This distribution is determined both by the geometrical properties of the porous medium and by the rheological properties of the fluid flowing through it. Taylor dispersion is negligible in most 3D porous media. Numerous studies have analyzed the parallel between disorder and dispersion in the case of Newtonian fluids [3–5]. At high Pe values, the stochastic velocity fluctuations lead to mechanical dispersion and result in an effective diffusion coefficient growing linearly with the Peclet number [6]. However, if stagnant zones are present, they may control longitudinal dispersion at very high Peclet number values. Fluid particles and tracers can only escape these stagnant regions by molecular diffusion. The coupling of velocity gradients and molecular diffusion defines hydrodynamic dispersion. In a pioneering work, Saffman [7] established that the longitudinal dispersivity (the ratio of the dispersion coefficient and the velocity) exhibits a logarithmic dependence on the Peclet number when disorder is only due to the random orientation of channels. Stagnant zones then correspond to the vicinity of pore walls or to channels nearly perpendicular to the mean flow direction. Baudet *et al.* [8] predict a similar singularity of the dispersion due to the low velocity near stagnation points of the flow field. Non-mechanical contributions that grow as $Pe \ln Pe$ and Pe^2 at high Pe, arise from a diffusive boundary layer near the solid surfaces and from regions of closed streamlines [6]. Experiments performed on non consolidated media show that the dispersion coefficient increases with an exponent slightly larger than 1 (around 1.2) with the velocity which may reflect a logarithmic correction [9].

Since Saffman's work, the effect of disorder on dispersion has been studied in three limiting cases; in the first case, the porous medium is homogeneous at large scales and heterogeneous at the pore scale resulting in large variations of the velocity. Porous media characterized by a bimodal pore-size distribution like packing of porous grains, are an example of such media. In this case, Koch *et al.* [6] have shown by taking into account retention inside particles that this hydrodynamic dispersion resulted

[a] e-mail: chaplain@versailles.inra.fr
[b] UMR CNRS n° 7608.

in a diffusivity increasing as Pe^2 at high Peclet values. In the second limiting case, the porous medium is heterogeneous at large scales and homogeneous at small scales like for instance, in stratified porous media [10,11]. More generally, when porous media are heterogeneous at any scale, then most of the flow should take place through a few preferential paths which would increase dispersion [12, 13]. This is the case when the distribution of permeability values is very broad. The correlation length of velocity may become much larger than the characteristic length (size of grains) of the porous medium [13], so that the mean-field approximation may be invalid [4,14].

Since a larger disorder of the porous media always results in an increase of dispersion, it has been suggested that the measurement of passive tracer dispersion may be a good tool to characterize heterogeneity [15].

On the other hand, few studies of tracer dispersion have dealt with non-Newtonian fluids. Their non linear rheological characteristics modify the velocity distribution in the pore space and thus influence tracer dispersion. Furthermore, experiments conducted on packings of porous grains have shown that the use of shear-thinning fluids increases the sensitivity of dispersion to heterogeneity [16].

In a previous paper, one of the authors showed that Saffman's approach can be extended to the case of a Bingham fluid [17]. Indeed, in the mean field approximation we used, we showed that the pressure gradient ∇P still satisfies Laplace's equation. The pressure gradient can be assumed to be uniform throughout the porous medium. The existence of a yield stress leads then to a cut-off in the orientation: flow takes place only in channels oriented at an angle from the mean velocity vector smaller than a critical value depending on the yield stress and on the pressure gradient. This results in a dependence of the longitudinal dispersivity on the yield stress that may be used to characterize experimentally the pore size distribution. However, non-Newtonian fluids of practical interest generally do not behave as simple Bingham fluids but exhibit a more complex behaviour [18]. For instance, polymer solutions are generally shear thinning, following a power law such as $0.2 \leq n < 1$ in an extended domain of shear rates currently ranging from 10^{-4} to $10^2\,\mathrm{s}^{-1}$ [19]. In particular, the shear-thinning effect dominates the rheological behaviour of semi-rigid polymer solutions [20–22].

In the following, we study the dispersion of passive tracers in a power-law fluid by considering the case where rheological characteristics of the the non-Newtonian fluid remain the same during all the dispersion measurement. This situation completely differs from other studies in which a non-Newtonian fluid displaces a Newtonian one (or the reverse). The shear viscosity, η, is then related to the local shear rate, $\dot{\gamma}$, by a power law: $\eta \propto \gamma n^{-1}$. The index n can be smaller than 1 (shear thinning fluids) or larger than 1 (shear thickening fluids). The value $n = 1$, corresponds to the case of a Newtonian fluid.

Only homogeneous porous media are considered, so that the length of decorrelation of fluid velocity may be assumed of the order of the channel length. This allows us to use the mean field approximation as introduced in Saffman's approach.

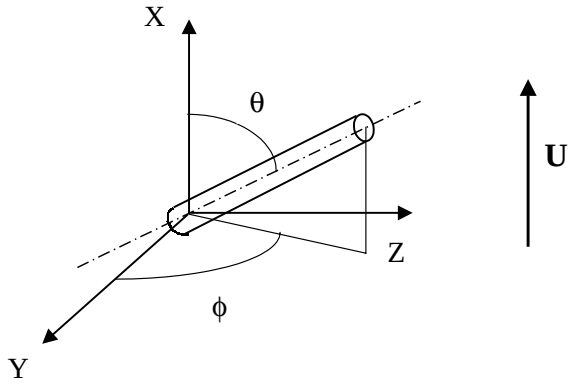

Fig. 1. The orientation of a pore is repaired by the angle θ and φ. The direction x is the direction of the mean flow of the fluid through the porous medium.

We also assume that the molecular diffusion of the tracer is independent of the fluid rheological properties. This has been verified by performing Taylor dispersion measurements, which is a classical tool to determine the molecular diffusion coefficient of small species [23,24]. Such measurements performed on capillary tubes [25] have shown that the molecular diffusion coefficient is not modified even for viscous concentrated polymeric solutions.

The situation described in the present paper corresponds typically to the case of a polymer solution of constant moderate concentration flowing in the porous medium and of a low molecular weight tracer such as ionic species or radioactive molecules. After describing calculations of the statistical properties of tracer displacement, we report analytical results on the flow properties and the dispersivity in a statistically homogenous and isotropic porous medium. We find that the dispersivity can be written as a function of the Peclet number and of the index n characterizing the power-law fluid. The scaling behaviour observed at large Peclet numbers and the crossover towards the Newtonian case already investigated by Saffman, are analyzed.

2 Modelling

As in Saffman's model, the porous medium is modelled as a set of randomly oriented cylindrical straight channels of length ℓ and radius a, the end of each channel being assumed to be connected to other channels at a pore. The channel orientation is characterized by angles θ and φ as indicated in Figure 1. The pressure gradient ∇P is assumed to be uniform throughout the porous medium. It is oriented along the x-axis as well as the average velocity U of the fluid. U, also called average interstitial velocity, is given by the spatial average over many pores

of the x-velocity component in individual channels:

$$U = \int_0^{\pi/2} \overline{\nu(\theta)} \cos\theta \sin\theta d\theta \tag{1}$$

where $\overline{\nu(\theta)}$ is the average speed inside a channel of orientation θ (*i.e.* the volume flow rate through the channel divided by its cross-section area). This average speed is calculated assuming that the motion of fluid is dominated by viscosity, the inertia of the fluid being negligible. The pressure difference ΔP between the ends of a given individual channel is a function of θ.

In a convective regime, $Pe > 1$, tracer dispersion is described as a random walk with non trivial properties. Saffman's approach consists in computing the probability distribution of the displacement of a single tracer particle after a given time T. Then, if the distance traveled is large enough so that paths of initially neighbouring particles become statistically independent, the dispersion of a cloud of particles can be deduced.

The probability distribution that the displacement of a single particle has a given value after a given time is an ensemble average over many realizations of the model porous sample. However, assuming ergodic hypothesis to be valid, this distribution also gives the proportion of fluid particles, which have a given displacement after a given time, average on the displacement of many particles throughout the same porous medium.

The path of a single fluid particle results from statistically independent steps, each one corresponding to the transit through one channel. The displacement (X_m, Y_m, Z_m) of a single particle and the elapsed time T_m after m steps are defined using the following relationships:

$$\begin{aligned} X_m &= \sum_i \ell \cos\theta_i \\ Y_m &= \sum_i \ell \sin\theta_i \cos\varphi_i \\ Z_m &= \sum_i \ell \sin\theta_i \sin\varphi_i \\ T_m &= \sum_i \frac{\ell}{\bar{\nu}_i(\theta_i)} \cdot \end{aligned} \tag{2}$$

The average displacement and elapsed time computed over many realizations are related to the mean values over many pores by:

$$\overline{X_m} = m\ell\bar{x} \quad \overline{T_m} = m\frac{\ell}{\nu_0}\bar{t} \tag{3}$$

with

$$\bar{x} = \int_0^{\pi/2} \cos\theta p(\theta) d\theta \quad \bar{t} = \int_0^{\pi/2} t(\theta) p(\theta) d\theta \tag{4}$$

where $\bar{x}$ and $\bar{t}$ are now dimensionless variables defined with respect to the length ℓ of channels and to the average speed $\overline{\nu(0)} = \nu_0$ in the $\theta = 0$ direction and where $p(\theta)$ is the probability for a fluid particle to chose a direction θ.

As a consequence:

$$\frac{\overline{X_m}}{\overline{T_m}} = U \quad \frac{X_m}{T_m} \to U \text{ when } m \to \infty. \tag{5}$$

The latter equation assume that each individual particle has performed a representative sampling of all velocity orientations after a long enough time.

Assuming that all orientations are equiprobable, the probability for a fluid particle to chose a direction θ, when starting from a pore is proportional to the velocity in this direction:

$$p(\theta)d\theta = \frac{\overline{\nu(\theta)} \sin\theta d\theta}{\int_0^{\pi/2} \overline{\nu(\theta)} \sin\theta d\theta} \tag{6}$$

as $\sin\theta d\theta$ is the fraction of channels in the range θ to $\theta + d\theta$.

If the structure of the medium is such that channels may be considered as thin compared to their length, then it can be assumed that tracer concentration is uniform across the cross-section and that it is convected with the average speed $\overline{\nu(\theta)}$.

An upper cut-off time t_0, equal to the time characterizing molecular diffusion along the length ℓ of a channel is introduced and leads to the following rules determining the dimensionless duration of step i:

$$\begin{aligned} t_i(\theta_i) &= \frac{\ell}{\overline{\nu}(\theta_i)} \frac{\nu_0}{\ell} = \frac{\nu_0}{\overline{\nu}(\theta_i)} \quad \text{if} \quad t_i \le t_0 = \ell\nu_0/2D_m, \\ t_i(\theta_i) &= t_0 \quad \text{if} \quad t_i \ge t_0. \end{aligned} \tag{7}$$

It results a critical angle θ_0 such that $t_i(\theta_0) = t_0$ separating the θ domains where either expression is valid.

The variance σ_x^2 and σ_t^2 and covariance σ_{xt} of the random variables (X_m, T_m) are given by:

$$\overline{(X_m - \overline{X_m})^2} = m\ell^2\sigma_x^2 = m\ell^2 \int_0^{\pi/2} (\cos\theta - \bar{x})^2 p(\theta) d\theta \tag{8}$$

$$\begin{aligned} \overline{(T_m - \overline{T_m})^2} = \frac{m\ell^2}{\nu_0^2}\sigma_t^2 &= \int_0^{\theta_0} (t(\theta) - \bar{t})^2 p(\theta) d\theta \\ &+ \int_{\theta_0}^{\pi/2} (t_0 - \bar{t})^2 p(\theta) d\theta \end{aligned} \tag{9}$$

$$\begin{aligned} \overline{(X_m - \overline{X_m})(T_m - \overline{T_m})} &= \frac{m\ell^2}{\nu_0}\sigma_{xt} \\ &= \frac{m\ell^2}{\nu_0} \left(\int_0^{\theta_0} (\cos\theta - \bar{x})(t(\theta) - \bar{t}) p(\theta) d\theta \right. \\ &\left. + \int_0^{\theta_0} (\cos\theta - \bar{x})(t_0 - \bar{t}) p(\theta) d\theta \right) \end{aligned} \tag{10}$$

as the domain of θ has been divided in two different parts.

Saffman introduced two dimensionless random variables χ_m and τ_m:

$$\chi_m = \frac{X_m - \overline{X}_m}{\ell\sqrt{m}} \qquad \tau_m = \frac{T_m - \overline{T_m}}{\frac{\ell^2}{\nu_0^2}\sqrt{m}} \tag{11}$$

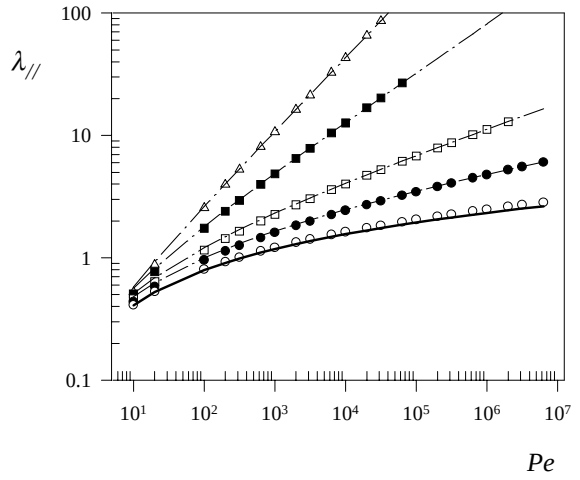

Fig. 2. Analytical results of the longitudinal dispersivity normalized by the pore length l, *versus* the Peclet number Pe. The solid line is Saffman's analytical solution obtained for the Newtonian case (Eq. (14)). Symbols are the complete exact solutions given in appendix for various values of the power-lax index n (○) 0.99, (●) 0.9, (□) 0.8, (■) 0.6, (△) 0.4. The broken lines are the approximated functions given in equation (21) with the corresponding index value.

which have a zero mean and variance and covariance values σ_x^2, σ_t^2 and σ_{xt} as defined in equations (8-10). The probability distribution of the number m of steps during the time T was then computed, where m is now a random variable $m(\tau;T)$ and T is fixed. Computing the longitudinal displacement X of a single particle after time T from equation (11):

$$X = \ell\sqrt{m}\chi_m + m(\tau,T)\ell\bar{x} \tag{12}$$

and assuming that the probability distribution of χ_m and τ_m approximated that of $\chi_{\overline{m}}$ and $\tau_{\overline{m}}$ at high m values, the general expression of the normalized longitudinal dispersivity $\lambda_{//}$ can be written:

$$\lambda_{//} = \frac{D_{//}}{U\ell} = \frac{1}{2\bar{x}}\left(\sigma_x^2 - 2\frac{U}{\nu_0}\sigma_{xt} + \frac{U^2}{\nu_0^2}\sigma_t^2\right). \tag{13}$$

In the case of a Newtonian fluid, the analytical function deduced from equation (13) is the logarithmic variation of the normalized dispersivity with Pe obtained by Saffman:

$$\lambda_{//} = \frac{1}{6}\ln\left(\frac{3Pe}{2}\right) - \frac{1}{24}. \tag{14}$$

This variation is represented by a continuous full line in Figure 2. At all Peclet number values, $\lambda_{//}$ remains small. For very large Peclet numbers greater than 10^7, $\lambda_{//}$ is of the order of 3. In the range of values generally encountered in experiments ($Pe \cong 10{-}1000$), $\lambda_{//}$ is close to 1.

Let us now generalize these calculations to the case of a power-law fluid. Due to the dependence of viscosity on the shear gradient, the velocity distribution inside the porous medium is modified. In channels with an angle θ with respect to U, the average speed is given by [18]:

$$\overline{\nu(\theta)} = \overline{\nu(0)}\cos\theta^{1/n} \quad \text{with } \overline{\nu(0)} = \frac{n}{3n+1}a\left(\frac{a\nabla P}{2K}\right)^{1/n} = \nu_0 \tag{15}$$

where K is the prefactor of the power law ($\eta = K\dot{\gamma}^{n-1}$) characterizing the non-Newtonian rheological characteristics of the fluid. From equations (4) and (15), we can then calculate the probability distribution $p(\theta)$:

$$p(\theta) = \frac{n+1}{n}\sin\theta\cos\theta^{1/n}. \tag{16}$$

For a shear thinning fluid ($n < 1$), since the effective viscosity is smaller in the channels where the velocity is large, and conversely larger in the channels where the velocity is small, the velocity distribution is widened by the non-Newtonian properties of the fluid. On the contrary, if the fluid is shear thickening ($n < 1$), then the non-Newtonian properties of the fluid lead to a narrowing of the velocity distribution.

3 Average velocity

Before considering tracer dispersion, it is interesting to investigate the properties of the mean average velocity U. From equations (1, 15), we find:

$$U = \frac{n^2}{(3n+1)(2n+1)}a^{(n+1)/n}\left(\frac{\nabla P}{2K}\right)^{1/n}. \tag{17}$$

The relationship between the average velocity U and the pressure gradient ∇P becomes non linear as soon as $n \neq 1$. Thus, in order to recover the usual Darcy's law, an effective viscosity depending on the flow rate has to be introduced; the permeability is always assumed to be independent of the rheological properties of the fluid flowing through the porous medium.

Most permeability measurement studies have dealt with shear thinning polymer solutions. The interpretation of data generally shows a good agreement with that expected from the power-law shear viscosity dependence [26–29]. However, several limitations have been encountered which will also arise in the case of tracer dispersion investigations. First, the power-law variation of the viscosity is observed to hold only in a finite range of shear rates. A Newtonian plateau region is often observed at low shear rates and at also large shear rates. Second, wall effects often appear when solutions of high molecular weight macromolecules flow in a porous medium [20,26,30]. Depending on the attractive or repulsive interaction between the macromolecules and the pore walls, the effective viscosity in the porous medium can be larger or, respectively, smaller than the viscosity measured with a rheometer. These walls effect are expected to be particularly important for small pore sizes. Third, at high flow rates, a large enhancement of the flow resistance appears above a well

defined low velocity threshold [26,31–33]. This latter deviation from the variation calculated for a power-law fluid arises from its time dependent properties and from the increase of elongational flow components due to rapid variations of the cross-section area of pore channels. Recent experiments performed on dilute solutions show that polymers then undergo a large conformation change and that an apparent "coil-stretch" transition takes place [33]. This effect is particularly important for large molecular weight polymers and large polymer concentrations [31,32]. It is to note that, in the case of rigid macromolecules, no flow resistance enhancement occurs and that, even at large flow rates, the observed behaviour agrees with that expected for a power-law fluid [34]. In the following, we do not consider these limitations and we assume that the fluid flowing inside the medium is well described by a power-law shear viscosity.

4 Dispersivity

The analytical expression of the dispersivity is calculated following the same procedure as Saffman. First we derive from equations (3, 5, 8-10) and (15) the statistical properties of the displacement and time distributions after m steps defined in equations (2) taking into account the angular probability distribution given by equation (16). The dispersivity is calculated using the general expression in equation (13). Calculations are straightforward and details are not reported here. The complete expressions are given in Appendix. Variations of the normalized dispersivity with the Peclet number are displayed in Figure 2 with double logarithmic scales. Each symbol refers to a given value of n as indicated on the plot; only the case of shear thinning fluids ($n < 1$) is considered here. The solid line corresponds to the logarithmic behaviour found by Saffman. As expected, we observe that, for a given value of the Peclet number, $\lambda_{//}$ increases for decreasing values of n. This is related as previously discussed, to the increase of the velocity distribution width due to shear thinning. In the limit of low Peclet numbers, all the curves collapse towards a same behaviour. In this limit, tracer dispersion is mainly due to molecular diffusion and thus is independent of the rheological properties of the fluid. Note that Saffman's model does not apply for $Pe \leq 1$. For a given value of n, $\lambda_{//}$ increases monotonously with the Peclet number. This variation is particularly fast for the smallest values of n demonstrating the large influence of shear thinning properties on tracer dispersion.

As the complete expression of $\lambda_{//}$ is quite long we looked for an approximate function λ_{app}. It can be seen in equation (13) that the dispersivity is the sum of three terms proportional respectively to σ_x^2, σ_{xt} and σ_t^2. The first one is constant and the second one decreases when the Peclet number increases. The dependence on the Peclet number is however dominantly controlled by the third one. We use thus the approximate value:

$$\lambda_{app} = \frac{1}{2\bar{x}} \frac{U^2}{\nu_0^2} \sigma_t^2. \tag{18}$$

The variance σ_t^2 is itself the sum of two terms (Eq. (9)). Assuming that the transit time distribution is broad, then the square of the average is negligible compared to the average of square. The first term can then be reduced to:

$$\int_0^{\theta_0} (t(\theta) - \bar{t})^2 p(\theta) d\theta = \int_0^{\theta_0} t^2(\theta) p(\theta) d\theta. \tag{19}$$

The second term is

$$\int_{\theta_0}^{\pi/2} (t_0 - \bar{t})^2 p(\theta) d\theta = (t_0 - \bar{t})^2 \cos\theta_0^{(n+1)/n}. \tag{20}$$

This term is constant for Newtonian fluids but increases with the Peclet number when $n \neq 1$. The following approximate expression of the dispersivity is then deduced from (Eqs. (19, 20)) as:

$$\lambda_{app} = \frac{n^2}{(n-1)(n+1)(2n+1)} \left[1 - \left(\frac{2n}{2n+1} \frac{1}{Pe} \right)^{n-1} \right]. \tag{21}$$

This approximate form λ_{app} fits very well the exact solutions over broad ranges of n and Peclet number values (the variations of λ_{app} with Pe are represented by broken lines on Fig. 2). The relative error $(\lambda_{app} - \lambda_{//})/\lambda_{//}$ is always smaller than 1%. Calculations show that this approximate function is also valid for $n > 1$, but obviously does not apply when $n = 1$.

For strongly non-Newtonian fluids ($n \leq 0.6$), the variation of the normalized dispersivity with the Peclet number indicates a power law dependence of $\lambda_{//}$ on Pe (the points fall on straight lines in the log-log representation of Fig. 2). An asymptotic power law with an exponent equal to $\alpha = 1 - n$ is also expected at high Peclet numbers from the approximate form given by equation (21). In order to analyze this point more quantitatively, we have computed the local slope α_{loc} of the curves of Figure 2 fitting $\log(\lambda_{//})$ *versus* $\log(Pe)$ to a linear variation within different ranges of the Peclet number. The results are reported in Figure 3 which displays the variation of α_{loc} with n. The solid line in Figure 3 is the theoretical relationship deduced from the approximate form: $\alpha = 1 - n$. This asymptotic regime is achieved at low Peclet numbers when $n \leq 0.6$ *i.e.* for strongly non- Newtonian fluids. On the contrary when n goes to 1, the asymptotic regime is only reached for very high values of the Peclet number (greater than 2×10^7 for $n = 0.9$). The displacement of the limit of validity of the power law approximation towards larger and larger Peclet numbers as n goes to 1 reflects the cross-over from a scaling behaviour for $n \neq 1$ towards a logarithmic behaviour for $n = 1$ (Newtonian fluid).

5 Conclusion

The generalization of Saffman's approach to the case of non-Newtonian power-law fluids allows to calculate the dispersion of a tracer in such fluids though a statistically

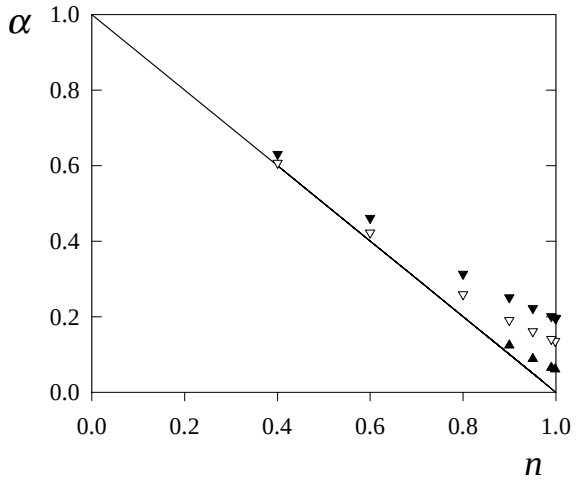

Fig. 3. Local slope of the longitudinal dispersivity as a function of the power law index of the fluid for three ranges of the Peclet number values. (▼) 100–200; (▽) 1000–2000; (▲) 10^7 to 2×10^7.

homogeneous porous medium. In the case of shear thinning fluids such as polymer solutions, a large enhancement of the dispersivity is predicted; this enhancement is particularly important for large values of the Peclet number and small values of the power-law viscosity exponent (strongly non-Newtonian fluids). We have derived an approximate expression which reproduces well the results of exact computations in an extended domain of Peclet numbers. Finally, we demonstrate that, for large Peclet numbers, the normalized dispersivity $\lambda_{//}$ follows a power law $\lambda_{//} \propto Pe^{1-n}$ in which n is the viscosity exponent. The extent of the range of Peclet numbers over which this law is valid depends on n: for small n values (strongly non-Newtonian fluids), it lower bound corresponds to Pe as small as 10, while, when n tends towards 1, this lower limit diverges to infinity. This is to be related to the transition to the logarithmic behaviour found for Newtonian fluids ($n = 1$).

The large enhancement of the normalized tracer dispersivity predicted for shear thinning fluids and its strong dependence on the rheological properties provide a good way to investigate the heterogeneities of porous media with enhanced sensitivity. Changing the power-law exponent of the viscosity can be easily done by changing the concentration of the polymer solutions and gives a tunable parameter allowing to obtain informations on the heterogeneity of the medium. Other rheological properties of the fluid such as the elongational viscosity, normal stress differences and non linear viscoelasticity may also play a role in dispersion and have to be considered in a further research [18].

Extensions of these calculations to model heterogeneous porous media (such as double porosity media) will be presented in a second paper. Considering the case of strongly heterogeneous porous media, the flow concentration in preferential channels should be enhanced while it will be reduced further in low velocity zones when shear-thinning fluids are involved. In particular, percolation like effects may be expected with a fluid with a well defined flow threshold like Bingham fluids. Flow velocity fields with large correlation lengths may result in this case but such problems are expected to be important only for extremely broad distributions of apertures of individual channels as is the case for instance in fractured media.

Appendix

The following expressions are the results of exact calculations of the different terms given by equations (5, 8-10). All variables are dimensionless with respect to the length ℓ of channels and the average speed ν_0 inside a channel oriented in the $\theta = 0$ direction.

$$\bar{x} = \frac{n+1}{2n+1} \qquad \text{and} \qquad \bar{t} = \frac{n+1}{n}$$

$$\sigma_x^2 = \frac{n+1}{3n+1} - \frac{(n+1)^2}{(2n+1)^2}$$

$$\sigma_{xt} = \frac{n+1}{2n}\sin\theta_0^2 + \frac{n+1}{2n+1}\bar{t}(\cos\theta_0^{(2n+1)/n} - 1) + \frac{(n+1)^2}{n(2n+1)}(\cos\theta_0 - 1) - \frac{n+1}{2n+1}\bar{t}(\cos\theta_0^{(n+1)/n} - 1) + (t_0 - \bar{t})\frac{n+1}{2n+1}\cos\theta_0^{(2n+1)/n}) - \frac{(t_0-\bar{t})(n+1)}{2n+1}\cos\theta_0^{(n+1)/n}$$

$$\sigma_t^2 = \frac{n+1}{n-1}(1 - \cos\theta_0^{(n-1)/n}) + 2\bar{t}\,\frac{n+1}{n}(\cos\theta_0 - 1) + \bar{t}^2(1 - \cos\theta_0^{(n+1)/n}) + (t_0 - \bar{t})^2(\cos\theta_0 - 1)$$

with $\cos\theta_0 = \dfrac{1}{t_0^n}$ and $t_0 = \dfrac{2n+1}{2n}Pe$ where the Peclet number Pe is defined with respect to the average velocity U of the fluid.

References

1. J. Bear, *Dynamics of fluids in porous media* (Elsevier Publishing Co., New York, 1972).
2. F.A.L. Dullien, *Porous media, fluid transport and pore structure*, 2nd ed. (Academic Press, New York, 1991).
3. J.P. Hulin, Adv. Coll. Int. Sci. **49**, 47 (1994).
4. M. Sahimi, *Flow and transport in porous media and fractured rocks* (VCH, weinheim, 1995).
5. J. Koplik, S. Redner, D. Wilkinson, Phys. Rev. A **37**, 2619 (1988).
6. D.L. Koch, J.F. Brady, J. Fluid Mech. **154**, 399 (1985).
7. P.G. Saffman, J. Fluid Mech. **6**, 321 (1959).
8. C Baudet, E. Guyon, J. Phys. Lett. **46**, L991 (1985).
9. J.J. Fried, M.A. Combarnous, Adv. Hydrosci. **7**, 169 (1971).
10. J.P. Bouchaud, A. Georges, Phys. Rep. **195**, 127 (1991).
11. J.C. Bacri, N. Rakotomalala, D. Salin, Phys. Rev. Lett. **58**, 2035 (1986).

12. E. Charlaix, E. Guyon, S. Roux, Transp. Porous Media **2**, 31 (1987).
13. E. Charlaix, H. Gayvallet, Europhys. Lett. **16**, 259 (1991).
14. A.J. Katz, A.H. Thompson, Phys. Rev. B **34**, 8179 (1986).
15. L.W. Gehlar, C.L. Axness, Water Resour. Res. **19**, 161 (1983).
16. A. Paterson, A. d'Onofrio, C. Allain, J.P. Hulin, J. Phys. II France **6**, 1639 (1996).
17. V. Chaplain, P. Mills, G. Guiffant, P. Cesari, J. Phys. II France **2**, 2145 (1992).
18. R.B. Bird, R.C. Armstrong, O. Hassager, *Dynamics of polymeric liquids* (Wiley-Interscience Publication, New-York, 1987).
19. W.W. Graessley, Adv. Polym. Sci. **16**, 1 (1975).
20. K.S. Sorbie, Y. Huang, J. Colloid Interface Sci. **145**, 74 (1991).
21. S. Chakrabarti, B Seidl, J. Vorwerk, P.O. Brunn, Rheol. Acta **30**, 114 (1991).
22. G. Chauveteau, J. Rheology **26**, 111 (1982).
23. K.C. Pratt, W.A. Wakeham, Proc. R. Soc. London A **336**, 393 (1974).
24. E. Grushka, E.J. Kikta, J. Phys. Chem. **78**, 2297 (1974).
25. M. Vartuli, J.P. Hulin, G. Daccord, AIChE J. **41**, 1622 (1995).
26. J.G. Savins, Ind. Eng. Chem. **61**, 18 (1969).
27. R.H. Christopher, S. Middleman, Ind. Eng. Chem. Fundam. **4**, 422 (1965).
28. R.J. Marshall, A.B. Metzner, Ind. Eng. Chem. Fundam. **6**, 393 (1967).
29. M. Greaves, K. Patel, Chem. Eng. Res. Des. **63**, 199 (1985).
30. G. Chauveteau, M. Tirrel, A. Omari, J. Colloid Interface Sci. **100**, 41 (1984).
31. W.M. Kulicke, R. Hass, Ind. Eng. Chem. Fundam. **23**, 308 (1984).
32. S. Rodriguez, C. Romero, M.L. Sargenti, A.J. Muller, A.E. Saez, J.A. Odell, J. Non-Newtonian Fluid Mech. **49**, 63 (1993).
33. A.R. Evans, E.S. Shaqfeh, P.L. Frattini, J. Fluid Mech. **281**, 319 (1994).
34. A.C. Gamboa, A.J. Müller, A.E. Saez, *Proceedings of The Fourth European Rheology Conference*, edited by C. Darmstadt (Editions Verlag, 1994), p. 157.